Realization of Logically Labeled Effective Pure States for Bulk Quantum Computation

Lieven M. K. Vandersypen,[1,2,*] Costantino S. Yannoni,[2] Mark H. Sherwood,[2] and Isaac L. Chuang[2]

[1]*Solid State and Photonics Laboratory, Stanford University, Stanford, California 94305-4075*
[2]*IBM Almaden Research Center, San Jose, California 95120*

We report the first use of "logical labeling" to perform a quantum computation with a room-temperature bulk system. This method entails the selection of a subsystem that behaves as if it were at zero temperature—except for a decrease in signal strength—conditioned upon the state of the remaining system. No averaging over differently prepared molecules is required. In order to test this concept, we execute a quantum search algorithm in a subspace of two nuclear spins, labeled by a third spin, using solution nuclear magnetic resonance and employing a novel choice of reference frame to uncouple nuclei.

The extraordinary potential of quantum algorithms [1–5] to solve certain problems in fewer steps than the best known classical algorithms has recently been highlighted by the experimental demonstration of elementary quantum computations [6–11]. These experiments made use of nuclear spins, subject to a magnetic field, as quantum bits (qubits: 2-level quantum systems). Even though traditional quantum algorithms assume that all qubits are necessarily initialized in a pure state, typically the ground state, the experiments were carried out at room temperature and the spins were in a highly mixed state.

The use of room temperature nuclear spins for quantum computing relies on the ideas of Gershenfeld and Chuang [12] and Cory, Fahmy, and Havel [13] to convert the mixed thermally equilibrated state into an "effective pure" state, at the expense of a signal decay, exponential in the number of qubits. The density matrix of such a state is diagonal and proportional to the identity matrix, except that one of the diagonal elements is different from the others. Because states proportional to the identity matrix are not observable in NMR spectroscopy and do not transform under unitary operations, an effective pure state gives the signal and has the dynamical behavior of a pure state. Until now, the signal of an effective pure state has been extracted by adding the signals from differently prepared molecules, either in different locations using magnetic field gradients [13] or by time-sequential experiments [14].

Logical labeling offers a fundamentally different approach for creating effective pure states: a submanifold spanned by 2^k states is selected from the Hilbert space of n coupled spins, by conditioning upon the state of $n - k$

ancilla spins. Gershenfeld and Chuang [12] predicted that the structure in the density matrix at equilibrium can be exploited to make this subsystem behave as if it were in a pure state, even if the entire system is at room temperature. This concept of embedding was previously used to observe Berry's phase in NMR spectroscopy [15].

In this Letter, we report the experimental implementation of logical labeling by embedding an effective pure 2-qubit subspace within a 3-spin molecule. Control over the dynamical behavior of the two logically labeled qubits is facilitated by the "uncoupling frame," a novel method to remove the effect of undesired couplings on the spin dynamics within a subspace. We execute Grover's quantum search algorithm as a test of logical labeling and the uncoupling frame and study the preservation of the effective pure state after many operations.

The Hamiltonian of weakly coupled nuclear spins in a molecule in solution and subject to a strong magnetic field is well approximated by [16] ($\hbar = 1$)

$$\mathcal{H} = -\sum_i \omega_i I_{zi} + \sum_{i<j} 2\pi J_{ij} I_{zi} I_{zj} + \mathcal{H}_{\text{env}}, \quad (1)$$

where $2I_{zi}$ is the $\hat{z}$ Pauli operator and ω_i is the Larmour frequency of spin i. J_{ij} is the strength of the scalar spin-spin coupling and $\mathcal{H}_{\text{env}}$ represents coupling to the environment, which causes decoherence. For a 3-spin system at typical magnetic field strengths, the Boltzmann distribution describing the thermal equilibrium populations of the states $\{|000\rangle, |001\rangle, |010\rangle, |011\rangle, |100\rangle, |101\rangle, |110\rangle, |111\rangle\}$ (where 0 and 1 represent a spin in the ground and excited state, respectively) is dominated by the Zeeman energy shift $\pm\hbar\omega_i/2$ and, for homonuclear systems ($\omega_i \approx \omega, i = 1, 2, 3$), is well approximated by

$$\frac{1}{2^3}\{1 + 3a, 1 + a, 1 + a, 1 - a, 1 + a, 1 - a, 1 - a, 1 - 3a\}, \quad (2)$$

where $a = \hbar\omega/2k_B T \ll 1$, with $k_B T$ the thermal energy. The thermal equilibrium state is thus highly mixed. However, the observable signal from the subspace spanned by the states $|000\rangle, |011\rangle, |101\rangle,$ and $|110\rangle$ is the same as the

signal from a system in the state $|000\rangle$, to within a scaling factor. This subspace is thus in the effective pure state $|000\rangle$.

In order to simplify subsequent logical operations and to separate the signals of the effective pure subspace and its complement, the populations can be rearranged by a sequence of 1- and 2-qubit unitary operations to obtain

$$\frac{1}{2^3}\{1 + 3a, 1 - a, 1 - a, 1 - a, 1 + a, 1 + a, 1 + a, 1 - 3a\}. \quad (3)$$

Now the subspace $\{|000\rangle, |001\rangle, |010\rangle, |011\rangle\}$ is in an effective pure state. This subspace corresponds to the spins B and C conditioned on or *labeled* by the state of the first spin, A, being $|0\rangle$ (we will call this the $|0\rangle_A$ subspace). This procedure is called logical labeling [12] and, combined with removal of coupling to spin A for the remainder of the pulse sequence, allows 2-qubit quantum computations involving only the spins B and C.

We selected bromotrifluoroethylene dissolved in deuterated acetone (10 mol %) as the central molecule in our experiments, because the spin-1/2 ^{19}F nuclei have large J couplings and chemical shifts, as well as long coherence times, which makes it suitable for quantum computation [4,12]. The ^{12}C nuclei are nonmagnetic and the interaction of the spin-3/2 Br nucleus with the fluorine spins is averaged out due to fast Br relaxation [16]. The ^{19}F Larmour frequencies are ≈ 470 MHz (at 11.7 T) and the spectrum is first order, consisting of three well-separated quadruplets (as in Fig. 3), with $\omega_A - \omega_B/2\pi \approx 13.2$ kHz and $\omega_C - \omega_A/2\pi \approx 9.5$ kHz. The coupling constants are measured to be $J_{AB} = -122.1$ Hz, $J_{AC} = 75.0$ Hz, and $J_{BC} = 53.8$ Hz (see also [17]). Single-spin rotations are realized by applying a radio-frequency (rf) magnetic field, oscillating in the $\hat{x}$-$\hat{y}$ plane. To simultaneously address the four lines in one quadruplet without affecting the other two quadruplets, the envelope of the rf pulses is Gaussian shaped (more complex shapes could improve the results) and the rf power is adjusted to obtain pulses of ≈ 300 μs. Experiments were performed at IBM using an Oxford Instruments wide-bore magnet and a Varian $^{\text{UNITY}}$*Inova* spectrometer with a Nalorac triple resonance (H-F-X) probe.

The logical labeling step is implemented as follows. Comparison of Eq. (2) with Eq. (3) shows that the populations of the states $|001\rangle \leftrightarrow |101\rangle$ and $|010\rangle \leftrightarrow |110\rangle$ must be interchanged, while the remaining four populations must be unaffected. This requires a CNOT$_{BA}$ and a CNOT$_{CA}$, where CNOT$_{ij}$ represents a controlled-NOT which flips j if and only if i is in $|1\rangle$. Furthermore, the two CNOT gates commute and can thus be executed simultaneously, as shown in Fig. 1.

This sequence implements the CNOT gates only up to single-spin Z rotations, which suffices for a diagonal
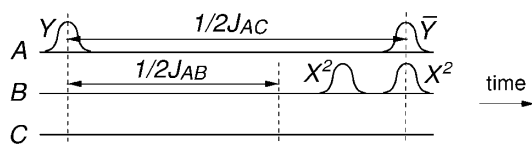
initial state as used here. Furthermore, the I_{zB}, I_{zC}, and $2I_{zB}I_{zC}$ terms in the Hamiltonian have no effect, since B and C remain along $\pm\hat{z}$. I_{zA} can be ignored because the pulses were applied in a reference frame in resonance with each spin. Figure 2 shows the measured populations of the eight basis states, before and after the sequence of Fig. 1. The results agree with the theoretical predictions of Eqs. (2) and (3).

The effective pure state prepared with logical labeling must remain pure throughout any subsequent computation. This requires that, while a computation is carried out using B and C, A must "do nothing," which is nontrivial in a system of coupled spins [19]: the effect of J_{AB} and J_{AC} must be removed. This could be done by using two refocusing X_A^2 pulses during every logical operation between B and C. We have devised a different method, which exploits the fact that it suffices to remove the effect of J_{AB} and J_{AC} *within the* $|0\rangle_A$ *subspace*. This uncoupling frame method requires no pulses at all and is described in Fig. 3.

Mathematically, the transformation of spin i's state from the laboratory frame to a reference frame rotating at $\omega_i + \Delta_i$ (with Δ_i the resonance offset frequency) is described by $|\psi\rangle = U|\psi'\rangle = \exp[i(\omega_i + \Delta_i)I_{zi}t]|\psi'\rangle$, where $|\psi'\rangle$ is the state in the new reference frame. After substituting $|\psi\rangle$ by $U|\psi'\rangle$ in the Schrödinger equation, and using the commutation rules between I_x, I_y, and I_z, it follows that $\mathcal{H}' = \mathcal{H} + \hbar(\omega_i + \Delta_i)I_{zi}$ [16]. Then, choosing $\Delta_B = -\pi J_{AB}$ and $\Delta_C = -\pi J_{AC}$ gives

$$\mathcal{H}' = 2\pi[(\mathbf{1}/2 + I_{zA})J_{BC}I_{zB}I_{zC} + (\mathbf{1}/2 - I_{zA})$$
$$\times (J_{BC}I_{zB}I_{zC} - J_{AB}I_{zB} - J_{AC}I_{zC})],$$

where $\mathbf{1}$ is the identity matrix. The first (second) term in the expression of $\mathcal{H}'$ acts exclusively on the $|0\rangle_A$ ($|1\rangle_A$) subspace. Any state within the $|0\rangle_A$ subspace evolves only under $J_{BC}I_{zB}I_{zC}$ and will remain within the $|0\rangle_A$ subspace. Within the $|0\rangle_A$ subspace and using the uncoupling reference frame, B and C are thus uncoupled from A. We experimentally confirm this by reconstructing the deviation density matrix [12] of the 3-spin system after creating the state $(|00\rangle + |11\rangle)/\sqrt{2}$ in the $|0\rangle_A$ subspace. Figure 4
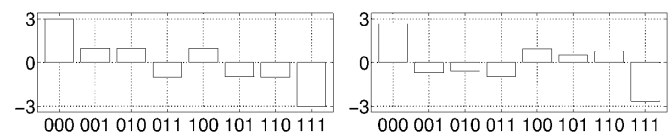

FIG. 1. The logical labeling pulse sequence. Y and $\bar{Y}$ denote a 90° rotation about the $\hat{y}$ and $-\hat{y}$ axis (right hand rule). X^2 are 180° rotations.

FIG. 2. Experimentally determined populations (in arbitrary units, and relative to the average) of the states $|000\rangle, \ldots, |111\rangle$ (left) in thermal equilibrium and (right) after logical labeling. The populations were determined by partial state tomography [18].
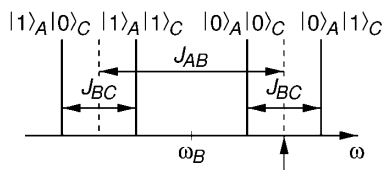
FIG. 3. Spectrum of the transitions of B, with the states of the other two spins as indicated. With respect to a reference frame rotating at $\omega_B/2\pi - J_{AB}/2$ (indicated by an arrow), spins B which see a spin A in $|0\rangle$ evolve under J_{BC} only and are thus *uncoupled* from A. J_{AB} does affect B's evolution in the $|1\rangle_A$ subspace, but the signal of this subspace does not interfere with that of the $|0\rangle_A$ subspace. Similarly, C's rotating frame must be moved to $\omega_C/2\pi - J_{AC}/2$. A separate channel was used for B and C. We note that the uncoupling frame is somewhat related to selective decoupling [20], a technique to determine the relative sign of J couplings by moving the reference frame of one nucleus (not several, as here) to the center of a submanifold.

shows the $|0\rangle_A$ subsystem in the predicted effective pure state and uncoupled from the $|1\rangle_A$ subspace.

The motivation for creating effective pure states is to provide a suitable initial state for quantum computation, and as a test of this we implement Grover's quantum search algorithm [3] on the two logically labeled spins, using the uncoupling frame. With this algorithm, one can find the unique but unknown x_0 which satisfies $f(x_0) = 1$, in $\mathcal{O}(\sqrt{N})$ queries of $f(x)$, where N is the number of possible entries x. Searching on a classical machine would require $\mathcal{O}(N)$ queries of $f(x)$. For $N = 4$, implemented here, a quantum computer finds x_0 in just one query, compared to on average 2.25 queries classically.
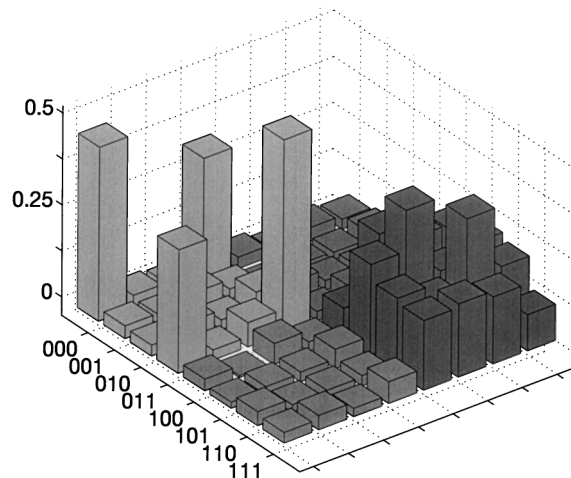

FIG. 4. Normalized experimental deviation density matrix (with the diagonal shifted to obtain unit trace for the effective pure state), shown in absolute value. The entries in the second quadrant are very small, which means that the $|0\rangle_A$ and $|1\rangle_A$ subspaces are uncoupled. The deviation density matrix is measured using quantum state tomography [18]; a series of 27 consecutive experiments with different sets of readout pulses (see below) permits one to determine all the components of the deviation from identity of the density matrix. The relative error in the state is $\|\rho_{\text{exp}} - \rho_{\text{th}}\|/\|\rho_{\text{th}}\| = 19\%$.

We use a pulse sequence similar to the one described in [6]. First, $Y_B Y_C$ rotates both spins from $|00\rangle$ into $(|00\rangle + |01\rangle + |10\rangle + |11\rangle)/2$, an equal superposition of the four possible inputs. The amplitude of the $|x_0\rangle$ term is then amplified in two steps [3]. First, one of four functions $f_{x_0}(x)$ is evaluated, flipping the sign of the $|x_0\rangle$ term. This is done by one of four conditional phase flips $Y_B Y_C - \Phi_B \Theta_C - \bar{Y}_B \bar{Y}_C - 1/2J_{BC}$, where $\Phi = X$ for f_{00} and f_{10} and $\Phi = \bar{X}$ for f_{01} and f_{11}. $\Theta = X$ for f_{00} and f_{01} and $\Theta = \bar{X}$ for f_{10} and f_{11}. Second, inversion about the average [3] is implemented by a Hadamard gate (a π rotation about an axis halfway between $\hat{x}$ and $\hat{z}$) on both spins, followed by the conditional phase flip corresponding to f_{00}, and another Hadamard gate. The pulse sequence for this inversion step can be reduced to $X_B X_C - Y_B Y_C - 1/2J_{BC} - \bar{Y}_B \bar{Y}_C$. The entire sequence for Grover's algorithm takes approximately 20 ms and the labeling step takes about 7 ms. The coherence time for the three ^{19}F spins, expressed as the measured transverse relaxation time constant $T_2 \approx 4$–8 s, is sufficiently long for coherence to be maintained throughout the labeling and computation operations.

The theoretical prediction is that the state of BC after completion of the algorithm is the effective pure state $|x_0\rangle$, which can be determined by a measurement of the spin states of B and C. This is done using a readout pulse for each spin, which rotates the spin back into the $\hat{x}$-$\hat{y}$ plane so that it generates a rotating magnetic field and induces an oscillating voltage in a pickup coil. The voltage is recorded with a phase sensitive detector, and Fourier transformed. The phase of the receiver is set to obtain a positive (negative) absorption line for a spin that was $|0\rangle$ ($|1\rangle$) before the readout pulse and is used to determine $|x_0\rangle$ (see Fig. 3). The experimental spectra (Fig. 5, left) as well as the deviation density matrices of the logically labeled subspace before, during, and after the computation, confirm that the state remains an effective pure state throughout the computation and that the final state is $|x_0\rangle$.

An interesting question is how many logical operations can be executed while preserving the effective pure character of the spins, and, further, how quickly errors accumulate during longer pulse sequences. We study this by iterating the conditional flip and inversion steps in Grover's algorithm, which ideally gives rise to a periodic pattern: for $N = 4$, the amplitude of the x_0 term is expected to be 1 after 1 iteration, and again after $4, 7, \ldots$ iterations [3]. Figure 5 demonstrates the expected periodic behavior in the output state in experiments with up to 37 iterations, which requires 448 pulses and takes about 700 ms. In addition to decoherence, errors mainly arise from imperfections in the pulses and coupled evolution during the 300 μs pulses (reduction of τ_1 and τ_2 partially compensated for this effect). Spectra of the quality of Fig. 5 were obtained by choosing a particular implementation of the composite $\hat{z}$ rotation in the phase flip step, such that the errors it introduces partially cancel
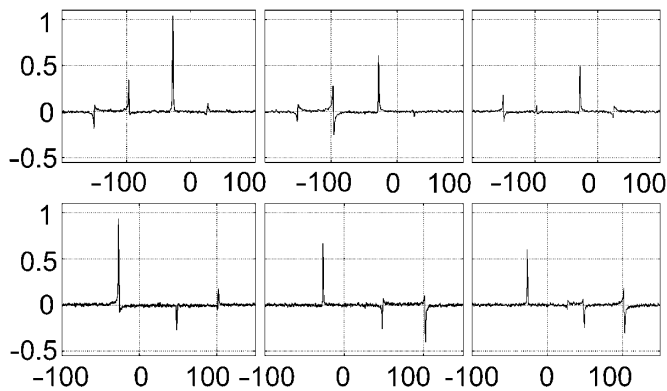
FIG. 5. Real part of experimental spectra (frequencies in the uncoupling reference frame) for spin B (top) and C (bottom), after executing Grover's algorithm 1 (left), 19 (center), and 37 (right) times, with $|x_0\rangle = |00\rangle$. The $|0\rangle_A$ subspace corresponds to the spectral lines at $\pm J_{BC}/2 = \pm 26.9$ Hz. Ideally, the line at -26.9 Hz is positive and absorptive, with unit amplitude, while the line at $+26.9$ Hz is zero. Even after 37 iterations, x_0 can be unambiguously determined.

with the errors of the inversion step. For example, while $YX\bar{Y}$, $\bar{Y}\bar{X}Y$, $X\bar{Y}\bar{X}$, and $\bar{X}YX$ are all mathematically equivalent, the errors may in practice add up or cancel out with the errors from previous or subsequent pulses. Clearly, a general optimization procedure will be very helpful for designing effective pulse sequences in future experiments involving more qubits.

We attribute the preservation of effective pure states during long pulse sequences in part to the use of the uncoupling frame, which provides an elegant and simple alternative to refocusing schemes involving π pulses. Multiple couplings with ancillae spins can be neutralized simply by moving the carrier frequencies of the computation spins by the appropriate $\sum \pm J/2$. In contrast, refocusing pulses would have to be applied during every single evolution interval and their complexity rapidly increases as more J couplings are to be refocused [19]. This technique may find application in future experiments using logical labeling, as well as in quantum error detection experiments [21], where the computation must proceed only within the subspace labeled error-free by the ancillae. However, refocusing pulses are still required when a coupling must be removed over an entire system rather than in a subspace only.

The present experiments demonstrate that a k-qubit room temperature system can behave as if it were very cold, except that the signal strength decreases exponentially with the number of qubits, when it is properly embedded in an n-spin system. The subspace dimension is limited by the number of equally populated states, which is $C_n^{n/2} = n!/(n/2)!^2$ in a homonuclear system, giving $k = \log_2(1 + C_n^{n/2})$. Thus, for large n, k/n tends to 1

($n = 40$ for $k = 37$). For heteronuclear spin systems, the analysis is more complex and k/n is generally smaller, but the number k of cold qubits that logical labeling can extract from n hot spins, as well as the number of operations required for logical labeling, still scale favorably.

*Email address: lieven@snow.stanford.edu
[1] D. Deutsch, Proc. R. Soc. London A **400**, 97–117 (1985).
[2] P. Shor, in *Proceedings of the 35th Annual Symposium on Foundations of Computer Science* (IEEE Computer Society Press, Los Alamitos, CA, 1994), pp. 124–134.
[3] L. K. Grover, Phys. Rev. Lett. **79**, 4709–4712 (1997).
[4] D. P. Divincenzo, Science **270**, 255–261 (1995).
[5] A. Ekert and R. Jozsa, Rev. Mod. Phys. **68**, 733–753 (1996).
[6] I. L. Chuang, N. Gershenfeld, and M. Kubinec, Phys. Rev. Lett. **80**, 3408–3411 (1998).
[7] I. L. Chuang, L. M. K. Vandersypen, X. Zhou, D. W. Leung, and S. Lloyd, Nature (London) **393**, 143–146 (1998).
[8] J. A. Jones and M. Mosca, J. Chem. Phys. **109**, 1648–1653 (1998).
[9] J. A. Jones, M. Mosca, and R. H. Hansen, Nature (London) **393**, 344–346 (1998).
[10] D. G. Cory, M. D. Price, W. Maas, E. Knill, R. Laflamme, W. H. Zurek, and T. F. Havel, Phys. Rev. Lett. **81**, 2152–2155 (1998).
[11] N. Linden, H. Barjat, and R. Freeman, Chem. Phys. Lett. **296**, 61–67 (1998).
[12] N. Gershenfeld and I. L. Chuang, Science **275**, 350–356 (1997).
[13] D. G. Cory, A. F. Fahmy, and T. F. Havel, Proc. Natl. Acad. Sci. U.S.A. **94**, 1634–1639 (1997).
[14] E. Knill, I. L. Chuang, and R. Laflamme, Phys. Rev. A **57**, 3348–3363 (1998).
[15] D. Suter, A. Pines, and M. Mehring, Phys. Rev. Lett. **57**, 242–244 (1986).
[16] A. Abragam, *The Principles of Nuclear Magnetism* (Clarendon Press, Oxford, 1961).
[17] D. D. Elleman and S. L. Manatt, J. Chem. Phys. **36**, 1945–1947 (1962).
[18] I. L. Chuang, N. Gershenfeld, M. G. Kubinec, and D. W. Leung, Proc. R. Soc. London A **454**, 447–467 (1998).
[19] N. Linden, H. Barjat, R. J. Carbajo, and R. Freeman, Chem. Phys. Lett. **305**, 28 (1998).
[20] J. F. Maher and D. F. Evans, Proc. Chem. Soc. **June**, 208–209 (1961).
[21] D. Leung, L. Vandersypen, X. Zhou, M. Sherwood, C. Yannoni, M. Kubinec, and I. Chuang, LANL e-print quant-ph/9811068 (to be published).